

# Selective and Random Syntheses of $[n]$ Cycloparaphenylenes ( $n = 8-13$ ) and Size Dependence of Their Electronic Properties

Takahiro Iwamoto,<sup>†</sup> Yoshiki Watanabe,<sup>†</sup> Youichi Sakamoto,<sup>‡,§</sup> Toshiyasu Suzuki,<sup>‡,§</sup> and Shigeru Yamago<sup>\*,†,§</sup>

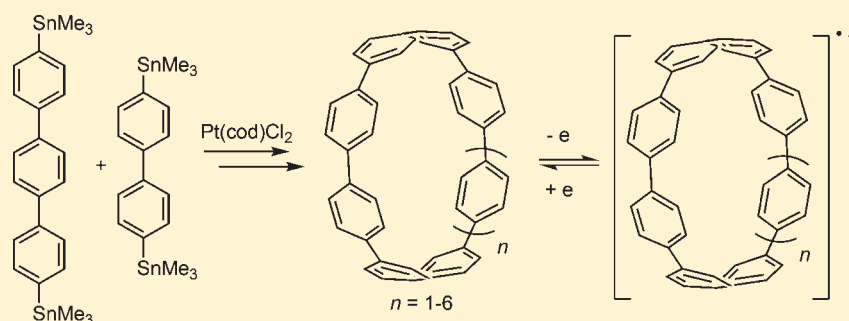
<sup>†</sup>Institute for Chemical Research, Kyoto University, Uji 611-0011, Japan

<sup>‡</sup>Institute for Molecular Science, Myodaiji, Okazaki 444-8787, Japan

<sup>§</sup>CREST, Japan Science and Technology Agency

**S** Supporting Information

## ABSTRACT:



$[n]$ Cycloparaphenylenes ( $n = 8-13$ , CPPs) were synthesized, and their physical properties were systematically investigated.  $[8]$  and  $[12]$ CPPs were selectively prepared from the reaction of 4,4'-bis(trimethylstannyl)biphenyl and 4,4''-bis(trimethylstannyl)terphenyl, respectively, with Pt(cod)Cl<sub>2</sub> (cod = 1,5-cyclooctadiene) through square-shaped tetranuclear platinum intermediates. A mixture of  $[8]$ – $[13]$ CPPs was prepared in good combined yields by mixing biphenyl and terphenyl precursors with platinum sources. Products were easily separated and purified by using gel permeation chromatography. In <sup>1</sup>H NMR spectra, the proton of the CPPs shifts to a lower field as  $n$  increased due to an anisotropic effect from the nearby PP moieties. Although the UV–vis spectra were rather insensitive to the size of the CPPs, the fluorescence spectra changed significantly in relation to their size. A larger Stokes shift was observed for the smaller CPPs. Redox properties of the CPPs were measured for the first time by using cyclic voltammetry, and the smaller CPPs had lower oxidation potentials. The results are consistent with the HOMO energies of CPPs, of which the smaller CPPs had higher energies.

## INTRODUCTION

Cycloparaphenylenes (CPPs) are hoop-shaped  $\pi$ -conjugated molecules, in which paraphenylene (PP) units are linked in a cyclic manner (Figure 1). Because of their unique structures, CPPs have attracted the attention of theoretical, physical, and synthetic chemists for more than a half-century.<sup>1–6</sup> In addition, they have recently gained much interest in material science and technology for photo-, electro-, and photoelectronic applications because they are the simplest structural unit of armchair carbon nanotubes (CNTs). Despite the potential impact of CPPs in fundamental and applied chemistry, science, and technology, their low availability has hampered the unveiling of their properties. Because properties of CNTs are strongly affected by the structure,<sup>7–9</sup> the effects of the size of CPPs on the properties would be of great interest.

Although CPPs have a simple structure, their synthesis has been a significant challenge.<sup>10,11</sup> After extensive efforts, Bertozzi<sup>12</sup> and Itami<sup>13–15</sup> have reported innovative synthetic methods to prepare  $[n]$ CPPs ( $n = 9, 12, 14, 15, 16$ , and 18). Both groups

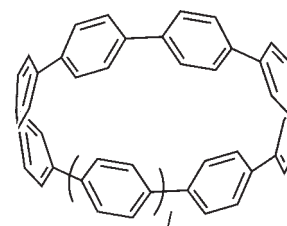
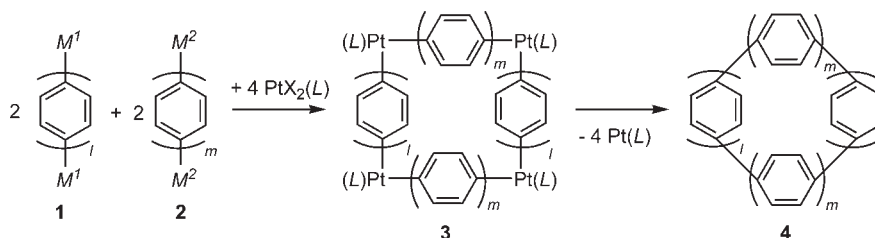


Figure 1. Structure of CPP.

utilize the sp<sup>3</sup>-hybridized carbon in cyclohexa-2,5-diene-1,4-diol or cyclohexane-1,4-diol derivatives, respectively, to induce the curvature required for the cyclic structure of CPPs, and the diol units are aromatized in the final step. Bertozzi has also reported that the fluorescence of CPPs is strongly affected by their size, and CPPs with smaller diameter exhibit larger Stokes shifts than

Received: March 15, 2011

Published: May 04, 2011

Scheme 1. Synthetic Route of  $[2(l + m)]$ CPP from Tetranuclear Platinum Complex

those of the larger CPPs among  $[n]$ CPPs ( $n = 9, 12, \text{ and } 18$ ).<sup>12</sup> The redox properties of CPPs are intriguing, but there are no reports of these properties so far.

We have been interested in the synthesis of CPPs by using a different strategy. We envisioned that quadrangular tetra(oligoparaphenylene)platinum complex **3** can serve as precursors for  $[2(l + m)]$ CPP **4** (Scheme 1). Because the bond angles of the substituents cis to each other in platinum complexes are  $\sim 90^\circ$ , **3** should form from appropriate linear oligoparaphenylene precursors, such as **1** and **2**, without inducing significant strain. Once **3** forms, multiple reductive eliminations of platinum from **3** would give **4**. When precursors with the same PP units are used ( $l = m$ ),  $[4l]$ CPP should selectively form from the square-shaped platinum complex. When the precursors have different PP units ( $l \neq m$ ), even CPPs should form from the rectangular platinum complex. Preliminary result revealed that  $[8]$ CPP, which is the smallest CPP so far synthesized, was selectively synthesized in excellent overall yield.<sup>16</sup> We report here details of the synthesis of CPPs by this route;  $[8]$  and  $[12]$ CPPs were selectively synthesized, and a mixture of  $[8]$ – $[13]$ CPPs was obtained in good combined yields.  $[10]$ ,  $[11]$ , and  $[13]$ CPPs were synthesized for the first time. All CPPs were isolated in pure form and fully characterized, and their photophysical and electrochemical properties were systematically studied. Redox properties of CPPs were obtained for the first time. The studies showed that not only the cyclic structure but also the size of the CPPs strongly affects their physical

properties. Full experimental details together with theoretical calculations to estimate the properties of CPPs are described.

## RESULTS AND DISCUSSION

**Structure, Strain Energy, and HOMO/LUMO Energies.** Structure and electronic properties of  $[n]$ CPPs ( $n = 4$ – $20$ ) were estimated by using density functional theory calculations at the B3LYP/6-31G\* level of theory. Although conformations and strain energies of several CPPs have recently been reported by Itami<sup>17</sup> and Bachrach,<sup>18</sup> their orbital energies have not been reported. Structures and strain energies of  $[17]$  and  $[19]$ CPPs were obtained for the first time. Structures and orbital energies of oligoparaphenylenes (OPPs,  $\text{H}[\text{C}_6\text{H}_4]_n\text{H}$ ) were also calculated as references.

All CPPs optimized in this study have conformations and Hartree–Fock energies virtually identical to those previously reported (see the Supporting Information).<sup>17,18</sup> The most stable conformation of even  $[n]$ CPPs is an alternating zigzag orientation of PP units with nearly  $D_{(n/2)h}$  point group symmetry, and that of odd CPPs is a helical arrangement of the PP units with  $C_1$  point group symmetry. Diameters, strain energies, and HOMO/LUMO energies of the CPPs are summarized in Table 1. We defined the diameter of the CPPs to be the diameter of a circle passed by the ipso-carbons of each PP unit. The diameter of the odd CPPs reported by Itami was smaller than our value by about 0.01–0.02 nm, whereas that of even CPPs is the same.

**Table 1.** Calculated Diameters and Strain and HOMO/LUMO Energies of  $[n]$ CPPs<sup>a</sup>

$n$	diameter <sup>b</sup> (nm)	strain energy <sup>c</sup> (kJ/mol) [kcal/mol]	HOMO energy (eV)	LUMO energy (eV)
4	5.70	602.7 [144.1]	−4.498	−1.990
5	7.05	490.5 [117.2]	−4.665	−1.955
6	8.40	406.8 [97.23]	−4.915	−1.780
7	9.77	356.5 [85.20]	−4.968	−1.802
8	11.13	307.1 [73.40]	−5.105	−1.699
9	12.49	279.6 [66.82]	−5.125	−1.720
10	13.87	246.6 [58.93]	−5.198	−1.666
11	16.61	229.4 [54.83]	−5.209	−1.677
12	16.61	205.21 [49.05]	−5.263	−1.632
13	17.99	194.33 [46.45]	−5.259	−1.651
14	19.36	176.14 [42.10]	−5.289	−1.638
15	20.74	168.33 [40.23]	−5.289	−1.638
16	22.11	153.82 [36.76]	−5.311	−1.622
17	23.49	148.27 [35.44]	−5.309	−1.630
18	24.87	136.63 [32.65]	−5.326	−1.617
19	26.23	132.76 [31.73]	−5.324	−1.622
20	27.62	122.96 [29.39]	−5.332	−1.621

<sup>a</sup>Data obtained from the DFT calculation at the B3LYP/6-31G\* level of theory. <sup>b</sup>Determined from the diameter of circle passed by the ipso-carbons of each PP unit. <sup>c</sup>A group equivalent reaction  $[(n + 1) \text{ terphenyl}] \rightarrow [n] \text{CPP} + n \text{ biphenyl}$  used for Itami<sup>17</sup> and Bachrach<sup>18</sup> was employed.

Strain energies of the CPPs at 0 K are within 0.4 kcal/mol of those obtained by Bachrach.<sup>18</sup> The strain energies of the CPPs increase with a decrease in the number of PP units, and there is a small but distinct odd–even effect, as pointed out by Bachrach. The strain energies of the odd CPPs are slightly higher than those expected from even CPPs. This effect is due to the existence of the helical conformation in the odd CPPs.

HOMO and LUMO energies of the CPPs increase and decrease, respectively, as the size of CPP decreases (Figure 2). The results are in sharp contrast to those of OPPs, of which the HOMO and LUMO energies increase and decrease, respectively, with an increase in the number of PP units due to an increase in the effective conjugation. The conflicting results for CPPs are due to the size dependence of the aromaticity of the PP units. The aromaticity of the PP units of CPPs tends to decrease, and the PP units tend to take a quinodimethane form rather than a benzenoid form when the number of PP units decreases.<sup>4,19–22</sup> Therefore, the smaller CPPs have stronger polyene character than do the larger analogues. The HOMO/LUMO energies of CPPs also exhibit odd–even effects. The HOMOs and LUMOs of the odd CPPs are higher and lower, respectively, than those expected from the even CPPs. The most probable explanation is the conformational differences of the odd and even CPPs as described above. The calculations suggest that the smaller CPPs have narrower HOMO–LUMO gaps than the larger CPPs and thus would be better lead compounds for electronic applications.

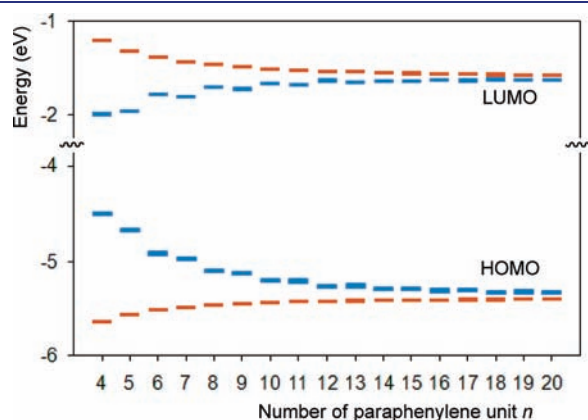


Figure 2. HOMO and LUMO energies of CPPs (blue) and oligoparaphenylenes (red).

HOMO–1 and HOMO–2 orbitals of  $[n]$ CPPs are completely or nearly degenerated in all cases, and the energies increase as the increase of the size of CPP. LUMO+1 and LUMO+2 orbitals are also completely or nearly degenerated except for  $[4]$ CPP, and the energies decrease with the increase of the size of CPP. In contrast to HOMO/LUMO energies, the size dependencies of these orbital energies are identical to those observed for OPPs (see the Supporting Information).

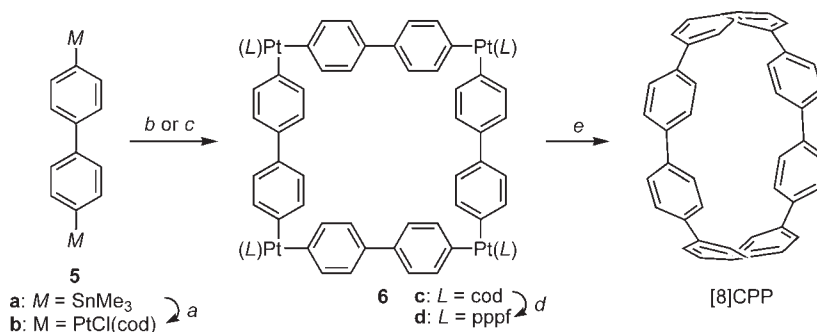
**Selective Synthesis of  $[8]$  and  $[12]$ CPPs.** Tetranuclear platinum complex **6c**, which is a precursor for  $[8]$ CPP, was prepared in a stepwise manner starting from 4,4'-bis(trimethylstannyl)biphenyl (**5a**).<sup>23</sup> Thus, **5a** was heated with 2 equiv of Pt(cod)Cl<sub>2</sub> (cod = 1,5-cyclooctadiene) in a refluxing THF/toluene to give bis-platinum biphenyl **5b** in 90% yield (Scheme 2). Next, **5b** was treated with 1 equiv of **5a** in 1,2-dichloroethane at 75 °C for 72 h to give **6c** in 34% yield. The same compound was also prepared in one step in 51% yield by mixing a 1:1 mixture of **5a** and Pt(cod)Cl<sub>2</sub> in 1,2-dichloroethane at 70 °C for 59 h. The yield increased to 84% when the reaction was carried out in refluxing THF for 36 h. Complex **6c** is less soluble and precipitates more easily from THF than from 1,2-dichloroethane. Thus, precipitation may shift the equilibrium for the formation of **6c** and also reduce the possibility of **6c** to transform into unwanted side products, such as linear oligomeric products, under thermodynamic conditions (see below).

The cod ligand in **6c** was substituted with 1,1'-bis(diphenylphosphino)ferrocene (dppf, 4.0 equiv) to give **6d** in 91% yield. Reductive elimination from **6d** forming  $[8]$ CPP proceeded in 49% yield by the addition of bromine (7.0 equiv)<sup>24</sup> and heating at 95 °C for 17 h in toluene.  $[8]$ CPP was prepared in three steps starting from **5a** in 37% overall yield. The <sup>1</sup>H NMR (7.48 ppm in CDCl<sub>3</sub>) and the <sup>13</sup>C NMR (127.6 and 137.8 ppm) and the MALDI TOF MS ( $m/z = 608.2504$ ) spectra are consistent with the structure of  $[8]$ CPP.

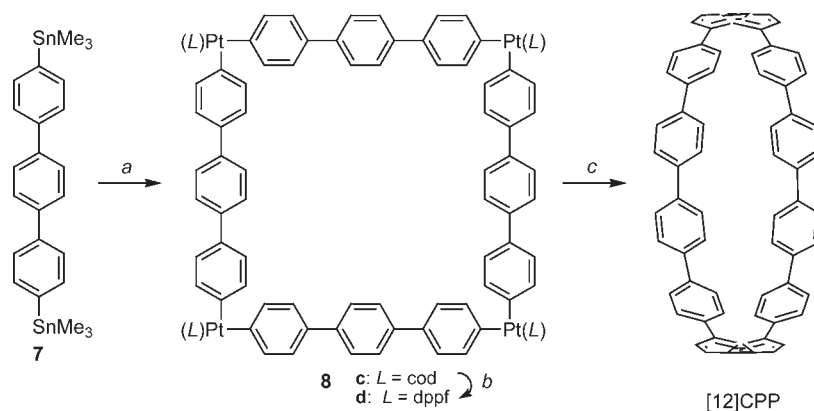
Addition of iodine (4.8%)<sup>25</sup> or triphenylphosphine (2.4%)<sup>26</sup> instead of bromide, or simple reductive elimination without additives (<2%), did not improve the efficiency of the reductive elimination. The ligand exchange reaction of **6c** with diphenylphosphinoethane, diphenylphosphinopropane, and xantphos proceeded smoothly to give the corresponding platinum phosphine complexes. However, reductive elimination of platinum from these complexes to  $[8]$ CPP did not proceed efficiently (<2% yield).

We next examined the synthesis of  $[12]$ CPP starting from 4,4'-bis(trimethylstannyl)terphenyl **7** (Scheme 3). The reaction of **7** with 1 equiv of Pt(cod)Cl<sub>2</sub> proceeded in refluxing THF, and

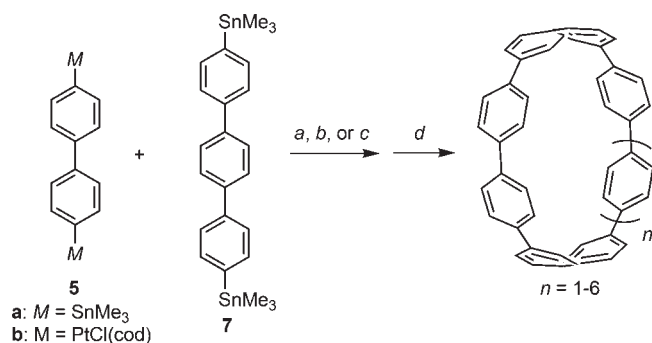
#### Scheme 2. Selective Synthesis of $[8]$ CPP<sup>a</sup>



<sup>a</sup> Conditions and reagents: (a) **5a**, Pt(cod)Cl<sub>2</sub> (2.0 equiv), THF/toluene, reflux, 10 h, 90%; (b) **5b**, **5a** (1.0 equiv), 1,2-dichloroethane, 75 °C, 72 h, 34%; (c) **5a**, Pt(cod)Cl<sub>2</sub> (1.0 equiv), THF, reflux, 36 h, 84%; (d) dppf (4.0 equiv), CH<sub>2</sub>Cl<sub>2</sub>, room temperature, 20 h, 91%; (e) Br<sub>2</sub> (7.0 equiv), toluene, 95 °C, 17 h, 49%.

Scheme 3. Selective Synthesis of [12]CPP<sup>a</sup>

<sup>a</sup> Conditions and reagents: (a) **7**, Pt(cod)Cl<sub>2</sub> (1.0 equiv), THF, reflux, 36 h, 20%; (b) dppf (4.3 equiv), CH<sub>2</sub>Cl<sub>2</sub>, room temperature, 36 h, 96%; (c) Br<sub>2</sub> (7.0 equiv), toluene, 95 °C, 17 h, 58%.

Scheme 4. Random Synthesis of [8]–[13]CPPs<sup>a</sup>

<sup>a</sup> Conditions and reagents: (a) **5b**, **7** (1.0 equiv), 1,2-dichloroethane, 50 °C, 32 h; (b) **5b**, **7** (1.0 equiv), 1,2-dichloroethane, 50 °C, 20 h; (c) **5a**, **7** (1.0 equiv), Pt(cod)Cl<sub>2</sub> (2.0 equiv), THF, reflux, 24 h; (d) dppf (2.0 equiv), CH<sub>2</sub>Cl<sub>2</sub>, room temperature, 13–15 h; Br<sub>2</sub> (2.0 equiv), toluene, 90–95 °C, 12–13 h. See main text for the yields of CPPs.

the desired platinum complex **8c** formed in 20% yield. The low yield may be due to the low solubility of oligoaryl platinum intermediates in THF. After ligand exchange from cod to dppf, the bromine-induced reductive elimination from the resulting platinum complex **8d** afforded [12]CPP in 58% yield. The yield for the reductive elimination step from **8d** to give [12]CPP was higher than that from **6d** to give [8]CPP due to the lower ring strain in [12]CPP. <sup>1</sup>H NMR (7.61 ppm in CDCl<sub>3</sub>), <sup>13</sup>C NMR (127.3 and 138.5 ppm), and MALDI TOF MS spectra (M<sup>+</sup> = 912.3754) were consistent with the data reported by Bertozzi<sup>12</sup> and Itami.<sup>13</sup>

**Random Synthesis of [n]CPPs (n = 8–13).** Encouraged by these results, we attempted to synthesize [10]CPP starting from bis(platinum)biphenyl **5b** and bis(stannyl)terphenyl **7** (1.0 equiv) by heating at 50 °C in 1,2-dichloroethane for 32 h (Scheme 4). The resulting mixture was treated with dppf (2.0 equiv to **5b**) without isolating the intermediate, followed by treatment with bromine (4.0 equiv). In the <sup>1</sup>H NMR spectrum of the crude mixture, five singlet signals in the range of 7.48–7.61 ppm were exhibited signals, indicating that there were five products. The products were easily separated by using size exclusion chromatography, and the products

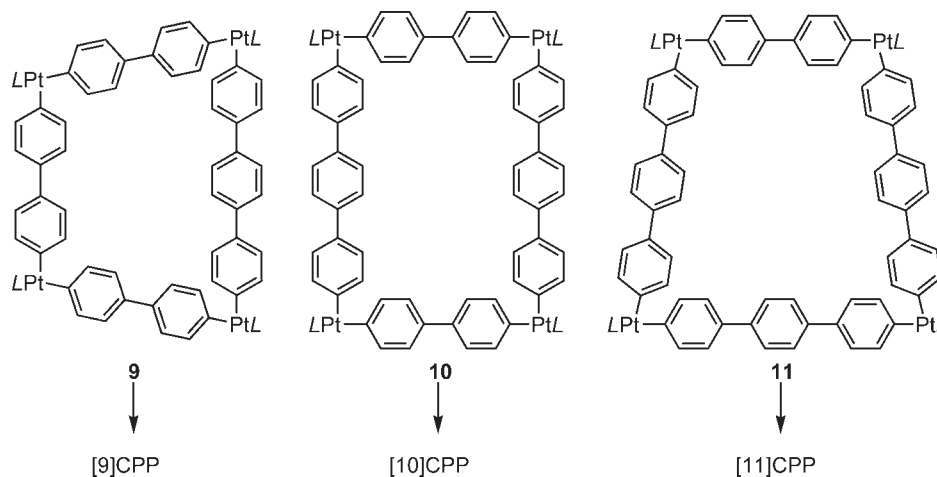
observed at 7.48, 7.52, 7.56, 7.58, and 7.61 ppm were determined to be [8], [9], [10], [11], and [12]CPP, respectively, by using MALDI TOF MS analysis. The overall yields of each compound from **5b** were 2.4%, 3.2%, 5.3%, 4.7%, and 2.3%, respectively.

The products and their ratio depended on the reaction conditions for the formation of the platinum complex. When **5b** and **7** were heated for 20 h under otherwise identical conditions, [9], [10], [11], [12], and [13]CPPs were formed in 5.4%, 9.6%, 7.7%, 3.8%, and 0.8% yields, respectively. [8]CPP was not observed. A mixture of CPPs was also obtained by mixing **5a**, **7**, and Pt(cod)Cl<sub>2</sub> in a ratio of 1:1:2 at 70 °C in 1,2-dichloroethane for 24 h. After the ligand exchange and bromine-induced reductive elimination reactions, [8]–[12]CPPs were obtained in 0.7%, 3.0%, 7.3%, 9.8%, and 3.7% yields, respectively.

[10]CPP should form from expected rectangular platinum complex **10**, and [8], [9], [11], and [12]CPPs should form from tetranuclear platinum complexes **6**, **9**, **11**, and **8**, respectively (Scheme 5). For [13]CPP to form, three terphenyl and two biphenyl units or one terphenyl and five biphenyl units must couple, indicating the formation of a penta- or hexanuclear platinum intermediate. It has already been reported that the transmetalation between arylstannanes and platinum is reversible and that the aryl-group on the diarylplatinum complexes undergoes scrambling.<sup>27</sup> Therefore, the formation of unexpected platinum complexes must be due to an equilibrium during the transmetalation and/or the ligand exchange reactions. Although the detailed mechanism is not fully understood, this synthetic route is attractive because it affords various CPPs, including odd CPPs, which can be easily separated by using GPC depending on their molecular size.

**NMR Spectroscopy of CPPs.** The <sup>1</sup>H and <sup>13</sup>C NMR chemical shifts of the CPPs, including the CPPs prepared by Bertozzi and Itami, are summarized in Table 2. A single peak in the <sup>1</sup>H NMR and two peaks in the <sup>13</sup>C NMR spectra were observed in all cases, indicating that the PP units freely rotate at room temperature on the NMR time scale. In the <sup>1</sup>H NMR spectrum, the chemical shift depends on the size of the CPPs and shifts downfield with an increase in the number of PP units, reaching a maximum at ~7.7 ppm (Figure 3). The chemical shift of the aromatic hydrogen in [n]paracyclophanes shows an opposite dependence on the size. The proton appears at lower magnetic field in smaller cyclophanes<sup>28–31</sup> due to a decrease in aromaticity and the deshielding effect caused by an increase in the strain. Therefore, the

Scheme 5. Possible Synthetic Precursors of [9], [10], and [11]CPPs

Table 2. Summary of  $^1\text{H}$  NMR,  $^{13}\text{C}$  NMR, and UV–Vis Spectral Data of  $[n]$ CPPs

$n$	$^1\text{H}$ NMR (ppm) <sup>a</sup>	$^{13}\text{C}$ NMR (ppm) <sup>a</sup>	UV (nm)/ $\epsilon$ ( $\text{M}^{-1} \text{cm}^{-1}$ )
8	7.48	127.60, 137.81	340/ $1.0 \times 10^5$
9	7.52 (7.53) <sup>b</sup>	127.51, 138.02 (127.4, 137.9) <sup>b</sup>	341/ $1.2 \times 10^5$
10	7.56	127.51, 138.29	341/ $1.3 \times 10^5$
11	7.58	127.40, 138.49	340/ $1.3 \times 10^5$
12	7.61 (7.62) <sup>b</sup> [7.61] <sup>c</sup>	127.33, 138.49 (127.3, 138.5) <sup>b</sup> [127.33, 138.52] <sup>c</sup>	339/ $1.4 \times 10^5$
13	7.64	127.49, 138.77	338/ $1.6 \times 10^5$
14 <sup>d</sup>	7.65	127.3, 138.8	— <sup>e</sup>
15 <sup>d</sup>	7.67	127.3, 138.8	— <sup>e</sup>
16 <sup>d</sup>	7.68	127.3, 138.9	— <sup>e</sup>
18 <sup>b</sup>	7.71	127.3, 139.0	$\sim 340$

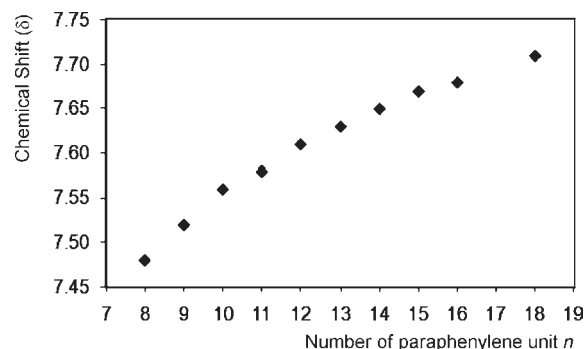
<sup>a</sup> Measured in  $\text{CDCl}_3$ . <sup>b</sup> Data taken from ref 12. <sup>c</sup> Data taken from ref 13. <sup>d</sup> Data taken from ref 14. <sup>e</sup> Not reported.

observed size dependence of the CPPs cannot be explained by the strain. It is possible that this trend is attributed to the difference in the anisotropic shielding effect of the adjacent PP units.

The  $^{13}\text{C}$  NMR chemical shifts also depend on the size of the CPPs. The peak for the ipso carbon atoms shifted downfield with an increase of PP units and reaches a maximum of  $\sim 139.0$  ppm, whereas the *ortho*- and *meta*-carbon atoms shift upfield, plateauing at  $\sim 127.3$  ppm.

**UV and Fluorescence Spectra of the CPPs.** The UV–vis absorption maxima ( $\lambda_{\text{max}}$ ) of the CPPs are summarized in Table 2. All of the CPPs absorb UV–vis light at around  $\lambda_{\text{max}} \approx 340$  nm regardless of their size (Figure 4), and the absorption coefficient ( $\epsilon$ ) slightly increased with an increase in the size of the CPP. The insensitivity of  $\lambda_{\text{max}}$  to the CPP size is consistent with results reported by Bertozzi,<sup>12</sup> but the results contradict the size dependence of the HOMO/LUMO gap discussed above.

To clarify this discrepancy, we carried out the time-dependent DFT calculation at the B3LYP/6-31+G\*\*/B3LYP/6-31G\* level of theory. The calculation reveals that the HOMO–LUMO transition is forbidden with no or very small oscillator strength in all cases, and that the strong absorption can be assigned to the sum of HOMO–2 to LUMO, HOMO–1 to LUMO, HOMO to LUMO+1, and HOMO to LUMO+2 transitions (see the Supporting Information). The results are consistent with the insensitivity of  $\lambda_{\text{max}}$  to the HOMO/LUMO gap of CPPs. The

Figure 3.  $^1\text{H}$  NMR chemical shift of  $[n]$ CPPs in  $\text{CDCl}_3$ .

small CPPs have small shoulder peaks at  $\lambda \approx 380$ – $450$  nm, and the absorptions may be related to the HOMO–LUMO transition.

All CPPs fluoresced, and the Stokes shift became larger with a decrease in the size of the CPP. The results are consistent with those reported by Bertozzi. The larger Stokes shift of the smaller CPPs can be explained by the release of strain energy in the excited state. Because smaller CPPs are more strained, they would undergo a larger structural change in the excited state than would the larger CPPs. All of the fluorescence spectra can be divided

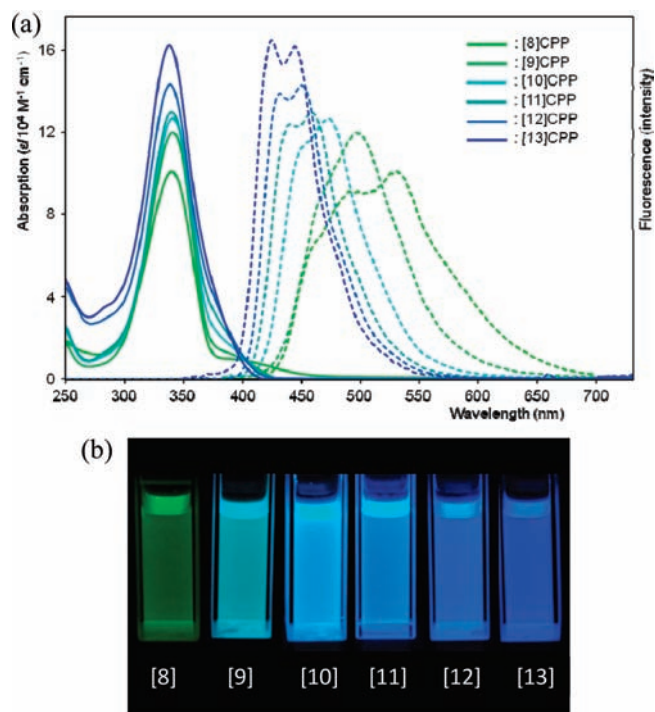


**Figure 4.** (a) UV-vis (—) and fluorescence (---) spectra and (b) fluorescence emission of [8], [9], [10], [11], [12], and [13] CPPs. Fluorescent spectrum is normalized to its UV-vis absorption intensity.

into two or three components. Further analysis of the UV-vis and fluorescence spectra is needed.

**Redox Properties of the CPPs.** Oxidation potentials of the CPPs were measured by using cyclic voltammetry (CV) in 1,1,2,2-tetrachloroethane solutions containing 0.1 mol/L of  $\text{Bu}_4\text{NPF}_6$  at room temperature. Voltammograms are shown in Figure 5, and the oxidation potentials are summarized in Table 3. Reduction wave(s) could not be observed within this solvent's potential window. All of the CPPs showed reversible oxidation waves, indicating that the oxidized intermediates are stable under the conditions used. The oxidation potential was strongly affected by the size of the CPPs, and [8]CPP has the lowest half-wave oxidation potential of 0.59 V (vs the ferrocene/ferrocenium couple). The oxidation potential increases as the size of the CPP increases, and the oxidation of [12] and [13]CPPs was at the edge of the solvent's potential window. However, a clear reversible oxidation wave was observed with a half-wave oxidation potential of 0.83 V for [12]CPP and 0.85 V for [13]CPP.

The oxidation potential increases monotonically with an increase in the number of PP units in the CPPs and reaches a plateau around 0.85 V. This trend is in good agreement with the trend in the HOMO energy of the CPPs. Although the HOMO energy shows odd-even effect, no such clear effect was observed in the oxidation potential (Figure 6). We believe that the results can be explained by considering the conformation of the CPPs. All of the PP units in CPP freely rotate on the basis of  $^1\text{H}$  and  $^{13}\text{C}$  NMR spectroscopy and are chemically equivalent at room temperature. However, the HOMO energies were calculated on the basis of the static structures with unequivalent PP units at 0 K. Because the HOMO energy is highly sensitive to the structure, the oxidation potential is likely to reflect the time-

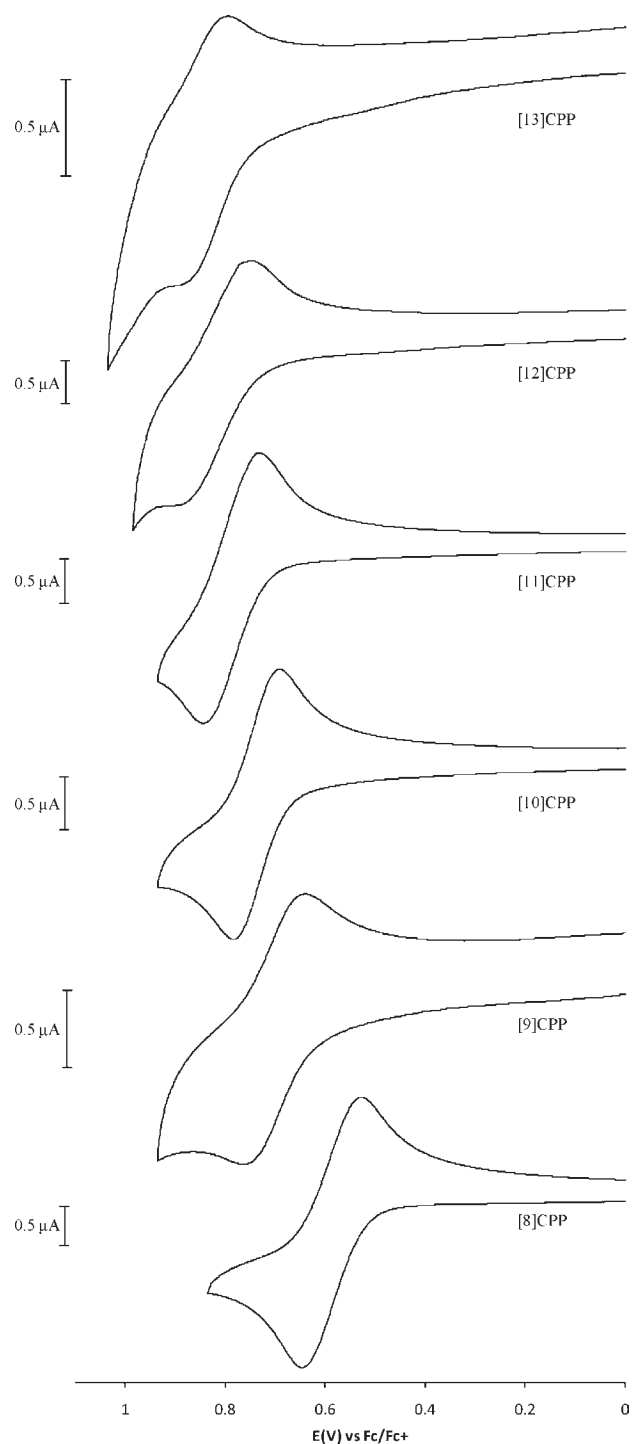


**Figure 5.** Cyclic voltammograms of CPPs in  $\text{Bu}_4\text{NPF}_6/\text{C}_2\text{H}_2\text{Cl}_4$  at room temperature.

averaged HOMO energy of the dynamic structures of the CPPs at room temperature. It is also possible that solvent plays some role because the calculation was carried out for molecules in a vacuum.

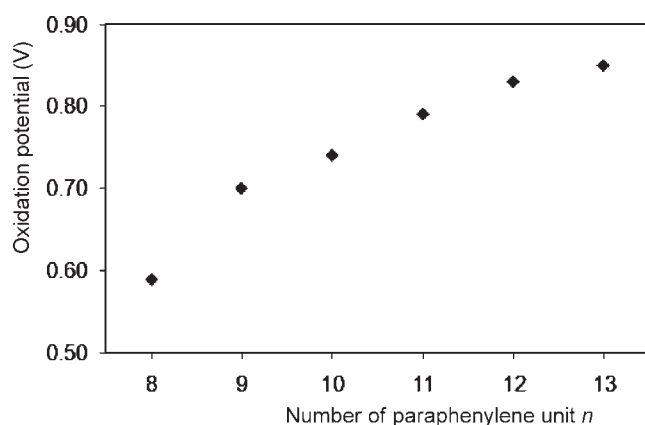
## SUMMARY

A new synthetic strategy for preparing CPPs through multi-nuclear arylplatinum complexes was successfully used for the

**Table 3. Half-Wave Oxidation Potential of  $[n]$ CPPs Obtained by Using Cyclic Voltammetry<sup>a</sup>**

$n$	$E$ (vs Fc/Fc <sup>+</sup> )
8	0.59
9	0.70
10	0.74
11	0.79
12	0.83
13	0.85

<sup>a</sup>V versus ferrocene/ferrocenium couple; Bu<sub>4</sub>NPF<sub>6</sub> (0.1 M) in 1,1,2,2-tetrachloroethane; scan rate = 20 mV/s; scan range = 0–1.25 V.

**Figure 6.** Correlation between oxidation potential and the number of PP unit of CPPs.

selective synthesis of [8] and [12]CPPs and the random synthesis of  $[n]$ CPPs ( $n = 8–13$ ). Although a mixture of CPPs was obtained in the latter case, they were easily separated by using gel permeation chromatography depending on their size. [10], [11], and [13]CPPs were synthesized and characterized for the first time. Except of [12]CPP, these CPPs have been difficult to prepare via other methods, which usually afford CPPs with  $n \geq 12$ . Therefore, this method is especially useful for the synthesis of CPPs with small sizes.

Experimental and theoretical studies clearly showed the effects of the cyclic structure and the size of the CPPs. The HOMO/LUMO gap of the CPPs shows an opposite trend to that of OPPs and decreases as the size of the CPP decreases. The oxidation potentials of the CPPs were determined for the first time, and all of the CPPs showed reversible oxidation waves. In addition, the oxidation potential depends on the size of the CPPs, and smaller CPPs have lower oxidation potentials. These results strongly suggest that small CPPs are attractive lead compounds in electronic applications. The size of the CPPs also strongly influences in fluorescence spectra of CPP, and the smaller CPP exhibits a larger Stokes shift. These results open a new possibility of CPPs for applications in optoelectronics.

## ■ ASSOCIATED CONTENT

**Supporting Information.** Synthesis and characterization of all new compounds, geometries and strain, and HOMO–2, HOMO–1, LUMO, and LUMO+1, and LUMO+2 energies of CPPs and OPPs determined by using the DFT calculation. This

material is available free of charge via the Internet at <http://pubs.acs.org>.

## ■ AUTHOR INFORMATION

### Corresponding Author

yamago@scl.kyoto-u.ac.jp

## ■ ACKNOWLEDGMENT

This work was partly supported from the Core Research for Evolution Science and Technology (CREST), Japan Science and Technology Agency. We thank Dr. Yasuyuki Nakamura of our group for valuable discussions and suggestions for the time-dependent DFT calculation and Prof. Norihiro Tokitoh and his group members of our institute for the measurement of fluorescence spectra. Computation time was provided by the Super Computer Laboratory, Institute for Chemical Research, Kyoto University.

## ■ REFERENCES

- (1) Schröder, A.; Meikelburger, H.-B.; Vögtle, F. *Top. Curr. Chem.* **1994**, *172*, 179–201.
- (2) Scott, L. T. *Angew. Chem., Int. Ed.* **2003**, *42*, 4133–4135.
- (3) Kawase, T.; Kurata, H. *Chem. Rev.* **2006**, *106*, 5250–5273.
- (4) Tahara, K.; Tobe, Y. *Chem. Rev.* **2006**, *106*, 5274–5290.
- (5) Steinberg, B. D.; Scott, L. T. *Angew. Chem., Int. Ed.* **2009**, *48*, 5400–5402.
- (6) Jasti, R.; Bertozzi, C. R. *Chem. Phys. Lett.* **2010**, *494*, 1–7.
- (7) Saito, R.; Dresselhaus, G.; Dresselhaus, M. S. *Physical Properties of Carbon Nanotubes*; Imperial College Press: London, 1998.
- (8) O'Connell, M. J. *Carbon Nanotubes: Properties and Applications*; Taylor & Francis: Boca Raton, FL, 2006.
- (9) Harris, P. J. F. *Carbon Nanotube Science: Synthesis, Properties and Applications*; Cambridge University Press: Cambridge, 2009.
- (10) Parekh, V. C.; Cuha, P. C. *J. Indian Chem. Soc.* **1935**, *11*, 95–100.
- (11) Friederich, R.; Nieger, M.; Vögtle, F. *Chem. Ber.* **1993**, *126*, 1723–1732.
- (12) Jasti, R.; Bhattacharjee, J.; Neaton, J. B.; Bertozzi, C. R. *J. Am. Chem. Soc.* **2008**, *130*, 17646–17647.
- (13) Takaba, H.; Omachi, H.; Yamamoto, Y.; Bouffard, J.; Itami, K. *Angew. Chem., Int. Ed.* **2009**, *48*, 6112–6116.
- (14) Omachi, H.; Matsuura, S.; Segawa, Y.; Itami, K. *Angew. Chem., Int. Ed.* **2010**, *49*, 10202–10205.
- (15) Segawa, Y.; Miyamoto, S.; Omachi, H.; Matsuura, S.; Šenel, P.; Sasamori, T.; Tokitoh, N.; Itami, K. *Angew. Chem., Int. Ed.* **2011**, *50*, 3244–3248.
- (16) Yamago, S.; Watanabe, Y.; Iwamoto, T. *Angew. Chem., Int. Ed.* **2010**, *49*, 757–759.
- (17) Segawa, Y.; Omachi, H.; Itami, K. *Org. Lett.* **2010**, *12*, 2262–2265.
- (18) Bachrach, S. M.; Stück, D. *J. Org. Chem.* **2010**, *75*, 6595–6604.
- (19) Viavattene, R. L.; Greene, F. D.; Cheung, L. D.; Majeste, R.; Trefonas, L. M. *J. Am. Chem. Soc.* **1974**, *96*, 4342–4343.
- (20) Kammermeier, S.; Herges, R. *Angew. Chem., Int. Ed. Engl.* **1996**, *35*, 417–419.
- (21) Kammermeier, S.; Jones, P. G.; Herges, R. *Angew. Chem., Int. Ed. Engl.* **1996**, *35*, 2669–2671.
- (22) Tsuji, T.; Okuyama, M.; Ohkita, M.; Imai, T.; Suzuki, T. *Chem. Commun.* **1997**, 2151–2152.
- (23) Curtis, M. D.; Allred, A. L. *J. Am. Chem. Soc.* **1965**, *87*, 2554–2563.
- (24) Yahav-Levi, A.; Goldberg, I.; Vignalok, A. *J. Am. Chem. Soc.* **2006**, *128*, 8710–8711.
- (25) Yahav-Levi, A.; Goldberg, I.; Vignalok, A.; Vedemikov, A. N. *J. Am. Chem. Soc.* **2008**, *130*, 724–731.

- (26) Shekhar, S.; Hartwig, J. F. *J. Am. Chem. Soc.* **2004**, *126*, 13016–13027.
- (27) Eaborn, C.; Odell, K. J.; Pidcock, A. *J. Chem. Soc., Dalton Trans.* **1978**, 357–368.
- (28) Ernst, L. *Prog. Nucl. Magn. Reson. Spectrosc.* **2000**, *37*, 47–190.
- (29) Wolf, A. D.; Kane, V. V.; Levin, R. H.; Jones, M., Jr. *J. Am. Chem. Soc.* **1973**, *95*, 1680.
- (30) Tobe, Y.; Takahashi, T.; Ishikawa, T.; Yoshimura, M.; Suwa, M.; Kobiuro, K.; Kakiuchi, K.; Gleiter, R. *J. Am. Chem. Soc.* **1990**, *112*, 8889–8894.
- (31) Jenneskens, L. W.; de Kanter, F. J. J.; Kraakman, P. A.; Turkenburg, L. A. M.; Koolhaas, W. E.; de Wolf, W. H.; Bickelhaupt, F.; Tobe, Y.; Kakiuchi, K.; Odaira, Y. *J. Am. Chem. Soc.* **1985**, *107*, 3716–3717.